Mansoura Engineering Journal

Volume 35 | Issue 4 Article 8

11-24-2020

Modeling and Simulation of Zafarana Wind Farm.

Sahar Kaddah
Dept. of Electrical Engineering, Faculty of Engineering, Mansoura University., Mansoura., Egypt

Mohamed Abdel-Wahab
Egyptian Electricity Transmission Co. EETC. Egypt

Recommended Citation
Kaddah, Sahar and Abdel-Wahab, Mohamed (2020) "Modeling and Simulation of Zafarana Wind Farm.," *Mansoura Engineering Journal*: Vol. 35 : Iss. 4 , Article 8.
Available at: https://doi.org/10.21608/bfemu.2020.125217

Mansoura Engineering Journal, (MEJ), Vol. 35, No. 4, December 2010. E. 14

Modeling and Simulation of Zafarana Wind Farm

نمذجة ومحاكاة مزرعة الرياح بالزعفرانة

Sahar S. Kaddah
Dept. of Electrical Engineering,
Faculty of Engineering,
Mansoura University

Mohamed N. Abdel-Wahab
Egyptian Electricity Transmission Co.
EETC, Egypt

ملخص البحث:

تصنف توربينات الرياح وفقا لاستراتيجية التحكم فيها إلى توربينات ذات سرعة ثابتة وتوربينات متغيرة السرعة. وتختلف استراتيجيات التحكم فى السرعة حسب تصميم ريشة التوربينة. وعلى حسب استراتيجية التحكم فى التوربينة يتم ربطها مع مولدات استنتاجية أو تزامنية أو مولدات استنتاجية مزدوجة التغذية. وتعتبرمزرعة الرياح بالزعفرانة والتي تصل قدرتها ٤٢٥ ميجاواط أكبر مزرعة (محطة) للرياح في الشرق الأوسط وأفريقيا. ويوجد بالمزرعة توربينات من كلا النوعين: ذات السرعة الثابتة والمتغيرة

فى هذا البحث تم استنباط نماذج رياضية فى حالة الاستقرار (steady state) للأنواع المختلفة من مولدات توربينات الرياح المستخدمة في مزرعة الرياح بالزعفرانة وتم استنباط هذه النماذج كدالة فى معامل الأداء وكل من القدرة الفعالة وغير الفعالة للمولدات المستخدمة، وقد تم التحقق من النماذج الرياضية المستبطة وذلك باستخدام البيانات المقاسة فى الموقع كمدخلات لها ومقارنة منحنيات القدرة الناتجة عنها بالنتائج الفعلية لتشغيل توربينات الرياح بالزعفرانة، وأثبتت المقارنة دقة هذه النماذج بحيث يمكن استخدامها فى مزيد من دراسات تشغيل الشبكات الكهربية المتضمنة توربينات الرياح. وقد تم تنفيذ برنامج تحليل تدفق القدرة على منطقة القناة وهى تمثل الجزء من الشبكة الكهربية المصرية الذى تدخل ضمنه مزرعة رياح الزعفرانة وذلك باستخدام النماذج الرياضية المستنبطة بحيث يتم محاكاة أداء الشبكة فى وجود توربينات الرياح ومن ثم استخدامه فى تقييم تأثير ربط مزرعة رياح الزعفرانة على استقرار الجهد بمنطقة القناة. وفى هذا البحث تم استنباط منهجية مقترحة لتقييم تأثير ربط محطات الرياح على استقرار جهد الشبكة وذلك بحساب الهامش المتوقع لاستقرار الجهد عند كل سرعة رياح واحتمال وقوع هذه السرعة مع تجميع سرعات الرياح المتوقعة.

ABSTRACT

The wind turbines are classified according to their control strategy to fixed speed and variable speed turbines. The most common control strategies are stall, pitch and active stall. Each control strategy is coupled to either squirrel cage induction generator, doubly fed induction generator or direct drive synchronous generator. Zafarana wind farm which has already reached a capacity of 425 MW is the largest installed wind farm in the Middle East and Africa. Both fixed and variable speed wind turbines are used in Zafarana wind farm.

This paper introduces steady state models of different types of Wind Turbine Generators (WTGs) used in Zafarana wind farm in terms of calculated performance coefficient, active power, and reactive power. The derived models are verified using actual data measured from the site as a very good approximation. So, they are used for further analysis. A complete power flow analysis of the Egyptian grid portion that contains Zafarana wind farm (Canal Zone that is represented by 34 bus system) is performed. Also the impact of interconnecting Zafarana wind farm on the Canal Zone voltage stability is evaluated by obtaining the expected voltage stability margin at each wind speed and accumulating for all expected wind speed values on the site.

Keywords*: *wind turbine modeling, voltage stability doubly fed induction generator, power flow, fixed speed wind turbines, variable speed wind turbines.

Accepted December 30, 2010.

1. Introduction

The rapid development of wind energy technology has significantly raised the penetration level of wind power in utility grids and consequently the wind turbines-grid integration. The wind turbines are classified according to their control strategy either fixed speed or variable speed. The most common control strategies are stall (based on the design of the blade), pitch (depends on pitch angle of the blade) and active stall (which is a combination of both). Fixed speed wind turbines (FSWT) are generally coupled with the utility grid through Squirrel Cage Induction Generator (SCIG) via capacitor banks. However, Variable Speed Wind Turbines (VSWT) are coupled with the grid through Doubly Fed Induction Generator (DFIG) via static converter in the rotor side or with synchronous generator.

The behavior of fixed speed-wind turbines in electrical power system and their interaction with both generation equipment and loads were studied in [1]. Transient behavior of grid connected FSWT and VSWT were studied in [2], while advanced tools for modeling, design and optimization of different types of wind turbines were studied in [3]. Equivalent wind farm models had been developed by aggregating wind turbines with identical incoming wind speed, and operating points on an equivalent electrical network [4]. In [5], proposed equivalent model for fixed speed wind turbines provided high accuracy for representing the dynamic response of wind farm on power system simulations was developed. In [6], modeling of wind farms with variable speed wind turbines based on aggregating the wind turbines in power system dynamic simulation were demonstrated. In [7], models for various types of WTGs compatible for grid-integration dynamic studies were established. Steady state models for FSWT and VSWT were presented to address the grid-wind turbines interaction in [8]. In [9], a dynamic model of a wind farm was used in addressing the dynamic interaction between a wind farm and a power system. The proposed model includes the substation where the wind farm is connected, the internal power collection system of the wind farm, the electrical, mechanical and aerodynamic models for the wind turbines. In [10] integrated models were built to enable the assessment of power quality and control strategies which implemented in commercial power system simulation tools.

This paper introduces models of different types of WTGs used in Zafarana wind farm in terms of calculated the performance coefficient, active power, and reactive power. These models are verified with the actual data measured from the site. A complete power flow analysis of the Egyptian grid portion that contains Zafarana wind farm is performed to measure different effects of Zafarana wind farm on the Egyptian grid.

2. Problem Formulation

This paper focuses on the wind energy conversion system (WECS) steady state model. The considered model includes the performance coefficient, active power, and reactive power of the WECS.

2.1. Performance Coefficient

The wind turbine performance coefficient C_p is the ratio between the mechanical power attracted from wind to the wind power; it can be expressed in a generic form as follows [8]:

$$C_p(\lambda,\beta)=C_1\left(\frac{C_2}{\lambda_i}-C_3\beta-C_4\beta^{C_5}-C_6\right)e^{\frac{-C_7}{\lambda_i}} \qquad (1)$$

Where:

$$\frac{1}{\lambda_i}=\frac{1}{\lambda+C_8\beta}-\frac{C_9}{\beta^3+1}$$

λ : Tip speed ratio of the rotor blade (tip speed compared with wind speed)

β : Blade pitch angle (rad)

C_1, C_2,….., C_9 are constant parameters depend wind turbine type.

The values of constants C_1 to C_9 vary according to the control strategy of the WECS, so that the above equation is valid for all types of WECS. Table 1 gives the values for these constants for different types of control strategy [11].

Table 1: Constants of Performance Coefficient of WECS

Control Strategy	Stall-FSWT	Pitch-FSWT	VSWT
C_1	0.5	0.44	0.73
C_2	116	125	151
C_3	0.4	0	0.005
C_4	0	0	0.002
C_5	0	0	2.14
C_6	5	6.94	13.2
C_7	21	16.5	18.4
C_8	0.08	0	-0.02
C_9	0.035	-0.002	-0.003

The mechanical power that can be extracted from a wind turbine is given by [11]:

$$P_m(v_w,\omega_r)=\frac{1}{2}\rho\, v_w^3 C_p(\lambda,\beta) \qquad \text{(2-a)}$$

Where: $$\lambda=\frac{\omega_r R}{v_w} \qquad \text{(2-b)}$$

P_m : Mechanical output power of the turbine (W)
ρ :Air density (kg/m^3)
A : Turbine swept area (m^2)
v_w : wind Speed (m/s)
ω_r : generator rotor angular speed (rad/sec)
R : Radius of the turbine blade (m)

2.2. Active and Reactive Power of FSWT

The induction generator output in terms of ω_r and the terminal voltage, V is obtained by using the equivalent circuit of the induction generator shown in Fig.1.

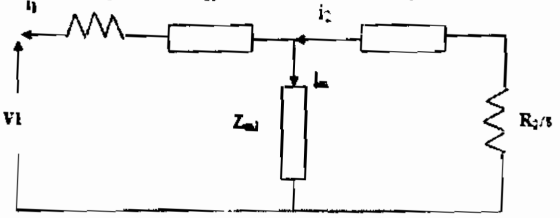

Fig. I: Equivalent Circuit of SCIG

The expressions for active and reactive power are obtained as [8]:

$$P_e=\frac{[R_1(R_2^2+s^2(X_m+X_{l2})^2+sR_2X_m^2)]|V|^2}{[R_2R_1+s(X_m^2-(X_m+X_{l2})(X_m+X_{l1}))]^2+[R_2(X_m+X_{l1})+sR_1(X_m+X_{l2})]^2}$$

$$Q_e=\frac{[X_mX_{l2}s^2(X_m+X_{l2})+X_{l1}s^2(X_m+X_{l2})^2+R_2^2(X_m+X_{l1})]|V|^2}{[R_2R_1+s(X_m^2-(X_m+X_{l2})(X_m+X_{l1}))]^2+[R_2(X_m+X_{l1})+sR_1(X_m+X_{l2})]^2}$$
(3-4)

P_e can be expressed as a function of the slip in a quadratic equation:

$$as^2+bs+c=0 \qquad (5)$$

Where,

$$a=P_eR_1^2(X_{l2}+X_m)^2+P_e(X_mX_{l2}+X_{l1}(X_{l2}+X_m))^2$$
$$-|V|^2R_1(X_{l2}+X_m)^2$$

$$b=2P_eR_1R_2X_m^2-|V|^2R_2X_m^2$$

and

$$c=P_eR_2^2(X_{l1}+X_m)^2+P_e(R_1R_2)^2-|V|^2R_1R_2^2$$

Then the slip is given by:

$$s=\min\left|\frac{-b\pm\sqrt{b^2-4ac}}{2a}\right|$$

Knowing the wind speed, active power P_e can be calculated. Then knowing slip s, reactive power Q_e can be computed using Equation (4) [8][12].

2.3. Active and Reactive Power of VSWT

In this type the VSWTs are coupled with the grid through either DFIG or synchronous generators. In case of coupling with DFIG, both stator and rotor are connected to the grid. The stator is connected directly to the grid whereas; the rotor is connected via static power converter (rectifier-inverter). This configuration has several advantages such as increasing capability of reactive power control, high conversion efficiency, high-performance regulating capability, low waveform distortion with little passive filtering and fast response to abnormal conditions.

The stator and rotor active and reactive power derived from the equivalent circuit of DFIG (see Fig. 2) are expressed by the following equations [13-14]:

$$P_S = 3R_s\left|\bar{I}_s\right|^2 + 3R_m\left|\bar{I}_{Rm}\right|^2 + 3\omega_1 \operatorname{Im}\left[\overline{\Psi}_m \bar{I}_r^{*}\right] \approx 3\omega_1 \operatorname{Im}\left[\overline{\Psi}_m \bar{I}_r^{*}\right] \qquad (6)$$

$$P_r = 3R_r\left|\bar{I}_r\right|^2 - 3\omega_1 s \operatorname{Im}\left[\overline{\Psi}_m \bar{I}_r^{*}\right] \approx -3\omega_1 s \operatorname{Im}\left[\overline{\Psi}_m \bar{I}_r^{*}\right] \qquad (7)$$

$$Q_S = 3\omega_1 L_{s\lambda}\left|\bar{I}_s\right|^2 + 3\omega_1 \operatorname{Re}\left[\overline{\Psi}_m \bar{I}_r^{*}\right] \qquad (8)$$

$$Q_r = 3\omega_1 s L_{r\lambda}\left|\bar{I}_r\right|^2 + 3\omega_1 s \operatorname{Re}\left[\overline{\Psi}_m \bar{I}_r^{*}\right] \qquad (9)$$

The air-gap flux (Ψ_m), stator flux (Ψ_s) and rotor flux (Ψ_r) are defined as [14]:

$$\overline{\Psi}_m = L_m(\bar{I}_s + \bar{I}_r + \bar{I}_{Rm}) \qquad (10)$$

$$\overline{\Psi}_s = L_{s\lambda}\bar{I}_s + L_m(\bar{I}_s + \bar{I}_r + \bar{I}_{Rm}) = L_{s\lambda}\bar{I}_s + \overline{\Psi}_m \qquad (11)$$

$$\overline{\Psi}_r = L_{r\lambda}\bar{I}_r + L_m(\bar{I}_s + \bar{I}_r + \bar{I}_{Rm}) = L_{r\lambda}\bar{I}_r + \overline{\Psi}_m \qquad (12)$$

where:

ω_1	Stator angular speed (rpm)
I_s	Stator Current (A)
I_r	Rotor current (A)
I_{Rm}	Active component of magnetizing current (A)
R_m	Magnetizing resistance (Ω)
R_s	Stator resistance (Ω)
R_r	Rotor resistance (Ω)
$L_{s\lambda}$	Stator leakage reactance (A)
$L_{r\lambda}$	Rotor leakage reactance (H)
L_m	Magnetizing reactance (H)

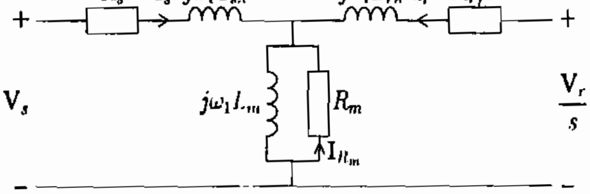

Fig. 2: Equivalent Circuit of the DFIG

Usual recommendations for most electric utility grids require values between 0.9 capacitive and 0.8 inductive power factors. The DC link in Fig. 3 is used for compensating reactive power. However, to obtain a specified power factor value at the point of connection, it is necessary to provide a significantly higher reactive power in the wind park to cover the reactive power compensation margin according to utility grid requirements taking into account transformers and transmission lines losses.

2.4. DFIG Static Converter

The basic model of the static converter is shown in Fig .3. On the AC side, the link is represented by two nodes r and i, whose voltages are $V_r\angle\theta_r$ and $V_i\angle\theta_i$, respectively. The AC currents at the rectifier and inverter terminals are denoted by $I_r\angle\phi_r$ and $I_i\angle\phi_i$, respectively. The tap changing transformers (off-nominal tap transformer) have tap ratios a_r and a_i, commutating reactance for rectifier and inverter side are X_{cr}, X_{ci}, the line voltage on the secondary side of the rectifier transformer is ($a_r V_r$) and the line current (I_r/a_r) [15].

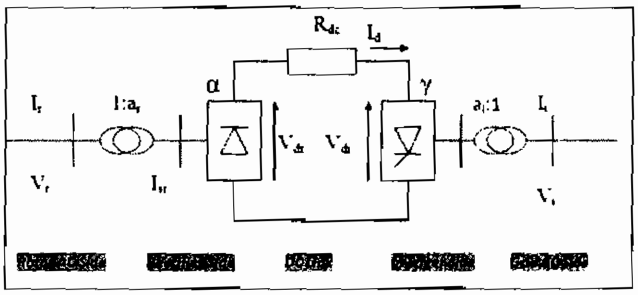

Fig. 3: Single line Diagram of DFIG Converter

The direct voltage at the rectifier terminal V_{dr} is given as [15]:

$$V_{dr} = (3\sqrt{2}/\pi)(a_r\bar{V}_r)\cos\alpha_r - 3(X_{cr}/\pi)\bar{I}_d \qquad (13)$$

Here α_r is the rectifier delay angle.The direct current I_d is related to the secondary AC line current thus: $I_{sr} = (\sqrt{6}/\pi)I_d$;

but $I_{sr} = (I_r/a_r)$; then $I_r = a_r(\sqrt{6}/\pi)I_d$

Applying of Kirchhoff's Voltage Law at DC link yields:

$$\bar{V}_{dr} - \bar{V}_{di} = \bar{I}_d R_{dc} \qquad (14)$$

The inverter voltage equation is given as:

$$\bar{V}_{di} = (3\sqrt{2}/\pi)(a_i \bar{V}_i)\cos\gamma_i - 3(X_{ci}/\pi)\bar{I}_d \tag{15}$$

where γ_i is the inverter extinction angle .

The power relations are given by:

$$\bar{V}_{dr}\bar{I}_d = \sqrt{3}\bar{V}_r\bar{I}_r\cos\phi_r \tag{16}$$

$$\bar{V}_{di}\bar{I}_d = \sqrt{3}\bar{V}_i\bar{I}_i\cos\phi_i \tag{17}$$

The AC line current on the inverter side is

$$\bar{I}_i = a_i(\sqrt{6}/\pi)\bar{I}_d \tag{18}$$

3. Modeling and Validation

Zafarana wind farm is the largest installed wind farm in the Middle East and Africa with a total capacity of 425 MW at the end of 2009 [16]. Zafarana wind farm include both FSWT stall regulated (Nordex 600/43) and FSWT pitch regulated (Vestas 660/47) and VSWT (Gamesa 850/52). In the following sections the steady state model of each type is derived using actual data measured from the site. Then, both active and reactive power curves are plotted and compared with the actual output values of the wind turbine.

3.1 Modeling and Validation of Stall Regulated FSWT

This type is aerodynamic braking control wind turbine coupled with squirrel cage induction generator in addition to shunt capacitor banks for reactive power compensation. In Zafarana farm there are 105 wind turbines (each Nordex-600 kW), with total rated power of 63 MW. The performance coefficient, C_p, is a function only of tip speed ratio, λ. By substituting in equation 2-a, power curve is constructed as illustrated in Fig .4. The developed power curve is compared with actual power curve of the Nordex 600 used in Zafarana wind farm. The comparison shows good closeness between the two curves. This means that the used model is a very good approximation model.

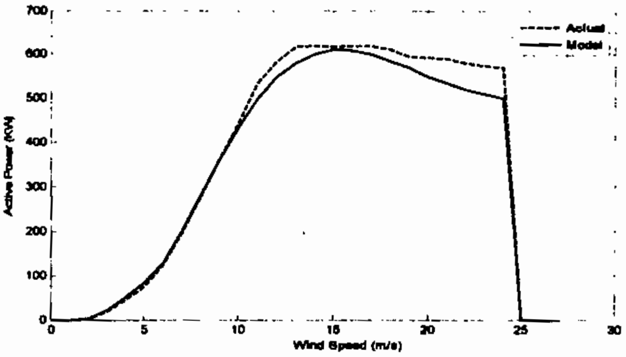

Fig.4: Actual and Developed Power Curve for Nordex 600

In this study the proposed model is applied for two cases; with and without compensation. Figure 5 depicts the reactive power curve for the two cases in addition to the reactive power curve of the actual normal operation state.

The results show that maximum power factor without compensation is 0.90 at rated wind speed but at low speed it may reach 0.69. Reactive power with compensation is given as a shunt capacitor bank 350 kVar, split into steps each 20 kVar which is mathematically controlled to provide reactive power to the system as calculated and illustrated in Fig. 5. Reactive power requirement at rated active power (rated speed) without/with compensation for both types is 290 and 122 kVar, respectively.

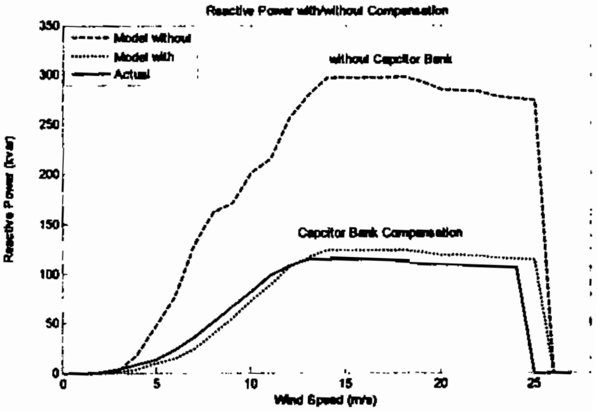

Fig.5: Nordex Wind Turbine Reactive Power

3.2. Modeling and Validation of Pitch Regulated FSWT

In this type, wind turbines are coupled with SCIG and also connected to shunt capacitor banks. In Zafarana farm there are 117 wind turbines (each Vestas - 660 kW), with total rated power of 77 MW. The performance coefficient C_p is a function of both tip speed ratio and pitch angle (λ and β). The power curve is constructed by substituting in equations (1 and 2) with altering the constants C_1 to C_9 to get the relation between C_p and λ and wind speed versus pitch angle β. The derived power curve is verified by comparing it with the actual power curve obtained from Zafarana wind farm as illustrated in Fig .6

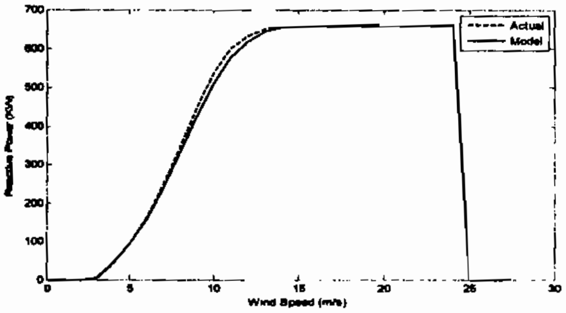

Fig. 6: Actual and Developed Power Curve for Vestas 660/47

Again the proposed model is applied to the previously mentioned two cases and the results are shown in Fig. 7. The results show that maximum power factor without compensation is 0.91 for Vestas pitch regulated at rated wind speed but at low speed it may reach 0.71. The reactive power compensation is the same as the one used in section 3.1. To keep the reactive power (rated speed) of the farm with fixed speed concept at 0.98 lag; the reactive power requirement is calculated and the results are illustrated in Fig. 7.

Comparing between the two FSWT types it can be observed that, without compensation the reactive power are 290 and 300 kVar for stall and pitch regulated type respectively. With capacitor bank compensation they are reduced to 122 and 134 kVar for the two types.

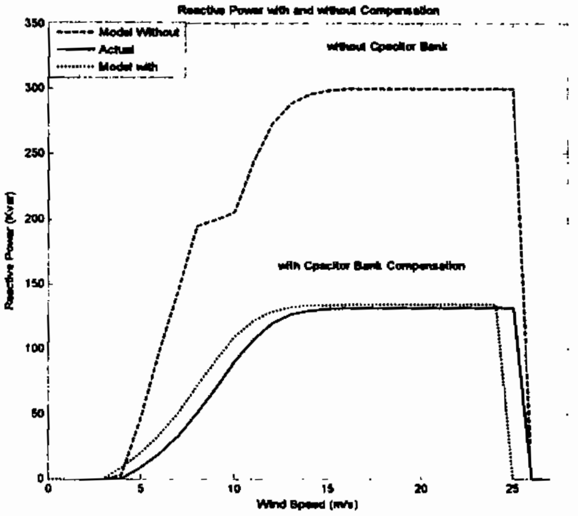

Fig.7: Vestas Wind Turbine Reactive Power With and without Compensation

3.3. Modeling and Validation of VSWT

In Zafarana farm there are 336 VSWT units, (each Gamesa 850 kW), with total rated power of 285 MW. These turbines are pitch regulated aerodynamic braking control coupled with DFIG in addition to a rotor ac-dc-ac converter. The performance coefficient, C_p is a function of both tip speed ratio and pitch angle (λ and β).

To match the rated power of the turbine, the angular speed ω is a margin between 14.6 to 30.8 rpm [16-17]. As the tip speed ratio is function of angular speed, the performance coefficient is calculated at each tip speed ratio for different values of angular speed within the above margin.

The power curve of the VSWT consists basically of two regions; first one starts at the cut-in wind speed and ends at rated wind speed where pitch angle is zero and shaft angular speed, ω, is optimum to capture maximum power. The second region starts at rated wind speed and continue up to cut-out wind speed where shaft speed is fixed and pitch angle varies to get smooth rated power as presented in Fig .8.

The DFIG generator feeds its electrical outputs (stator and rotor) into infinite bus-bar via static power ac-dc-ac converter in the rotor circuit through the variation of the firing angles α (0 -20^0) & γ (10 -30^0) of both rectifier and inverter respectively. Knowing active power of the rotor (P_r) and holding inverter terminal voltage (V_i) constant at 1 p.u., the reactive power output of the inverter (Q_r) and the input voltage of the rectifier (V_r) are calculated as a function of firing angles (α and γ) using the equations (6 to 18). The margin of reactive power of variable speed wind turbine at power factor 0.98 is illustrated in Fig .9.

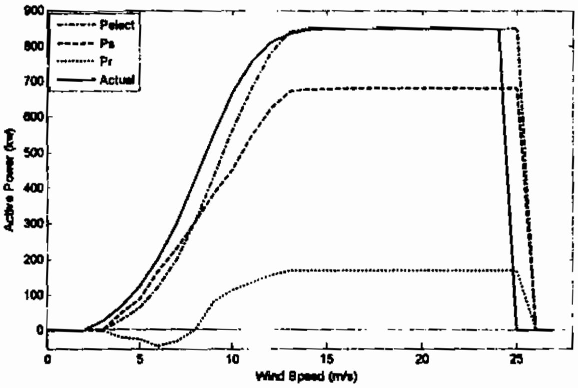

Fig. 8: Actual and Developed Power Curve for Gamesa 850/52

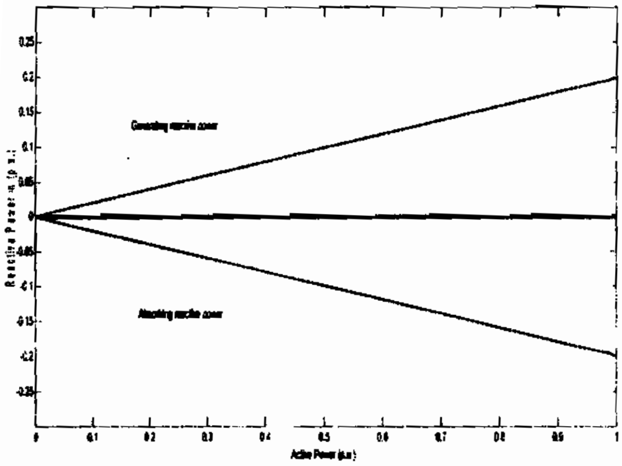

Fig. 9: Gamesa Wind Turbine Reactive Power Margin at pf = 0.98

3.4. Zafarana Wind Farm Output

For different wind speeds, the total active and reactive power delivered from Zafarana wind farm units are calculated using the proposed models according to the prescribed control strategies. The results are shown in Table 4.

4. Power Flow Analysis

To study the impact of the Zafarana wind farm on the Egyptian utility grid, a power flow analysis is performed. In load flow studies, the bus that contains the FSWT only is considered as a load bus (P-Q bus), whereas the bus that contains the VSWT only is considered as a voltage control bus (P-V bus). In case that both types are connected on the same bus, the FSWT output is considered as a negative load and the bus itself is considered as a voltage control bus under the effect of the VSWT insertion.

4.1. Canal Zone Description

Zafarana wind farm is part of the Canal Electricity Zone, which is one of the five areas that form the Egyptian electricity network. Canal Zone is represented by a 34- bus system; ten of them are generating bus. Tables A1 and A2 depict bus and line data of that zone.

Zafarana wind farm provides 425 MW at rated wind speed supported by two grand power stations, Ataka power station 2*415 & 2*185 MW and Gulf power station 2*420 MW. The two stations are considered as a backup for severe wind conditions [18]

4.2. Power Flow Results

To perform power flow analysis for the canal electricity zone including Zafarana wind farm, the fixed speed wind farm (140 MW) is considered as a P-Q bus where it provides 140 MW and consumed 28 MVar from the grid at rated wind speed. While the variable speed wind turbines (285 MW) modeled as PV bus provides the grid with 285.6 MW and reactive power margin of ± 57MVar.

The output results of performing power flow program for the Canal Zone 34-Bus System are listed in Tables 5 and 6. Bus voltage (magnitude and angle), active and reactive power for all buses are shown in Table 5. While the output line results are listed in Table 6. The power flow program is implemented for rated wind speed (13 m/s). The program with the proposed wind turbine models can be executed for any wind speed up to the furling speed (25 m/s).

Table 2: Calculated Power Curve for Gamesa 850/52

Wind Speed (m/s)	N (rpm)	Slip s (%)	ω_r (rpm)	P_s(kW)	P_r (kW)	P_e (KW)
16-25	30.8	-0.26	1.26	680	170	850.0
15	30.8	-0.26	1.26	679.2	169.8	849.0
14	30.8	-0.26	1.26	678.4	169.6	848.0
13	30.8	-0.26	1.26	672	168	840.0
12	30.8	-0.26	1.26	623.9	156,0	779.9
11	30.8	-0.26	1.26	547.7	136.9	684.6
10	30.8	-0.26	1.26	451.6	112.9	564.5
9	27.5	-0.13	1.13	387.1	48.4	435.5
8	24.3	0	1	307.0	0.0	307.0
7	21	0.13	0.87	233.3	-30.3	203.0
6	17.84	0.26	0.74	166.2	-43.1	123.1
5	14.6	0.39	074	88.0	-50	65.2
4	14.6	0.52	0.6	43.0	-56	27.9

Table 3: Calculated Reactive Power Curve for Gamesa 850/52

wind Speed (m/s)	rpm	Slip S [%]	Power Factor total		Q_s (kVar)		Q_r (kVar)		Q_t (kVar)	
			min	max	min	max	min	max	min	max
16-25	30.8	-0.26	0.95	0.98	226	521.7	17.8	104.3	240	626
15	30.8	-0.26	0.95	0.98	224	515.6	16.5	101.7	239	617
14	30.8	-0.26	0.94	0.98	221	508	15.2	99.1	234	604
13	30.8	-0.26	0.94	0.98	204	486.3	13.5	84	218	552
12	30.8	-0.26	0.93	0.98	187	426	11.3	69.5	198	496
11	30.8	-0.26	0.93	0.98	157	358	9.6	47	167	405
10	30.8	-0.26	0.92	0.98	126	289	7.8	25.2	134	314
9	27.5	-0.13	0.92	0.98	105	240	2.8	19.2	110	259
8	24.3	0	0.91	0.98	82.6	190	0	0	82.6	189.5
7	21	0.13	0.91	0.98	61	139	-10	-20	40.7	119
6	17.8	0.26	0.90	0.98	46	88.7	-7.4	-16.1	38.3	72.6
5	14.6	0.4	0.90	0.93	30.4	70	-4.6	-9.2	25.8	60.3

Table 4: Zafarana Wind Farm Output

Wind Speed m/s	Fixed Speed				Variable Speed		Total Active Power
	Nordex 105*600 kW		Vestas 117*660 kW		Gamesa 477*850 kW		
	P(MW)	Q(MVar)	P(MW)	Q(MVar)	P(MW)	Q(MVar)	P(MW)
3	0.21	-0.042	0.0	0.0	0.0	0.0	0.210
4	1.785	-0.357	0.339	-0.068	9.2	±1.8	11.324
5	4.725	-0.945	5.121	-1.024	21.4	±6.22	31.246
6	7.57	-1.514	11.306	-2.261	45.5	±11.743	64.376
7	13.02	-2.60	19.410	-3.882	66.8	±19.366	99.23
8	20.58	-4.116	29.446	-5.893	79.9	±23.147	129.9
9	29.085	-5.817	40.926	-8.185	143.2	±41.50	213.185
10	38.22	-7.644	52.623	-10.524	185.8	±53.853	276.643
11	46.62	-9.324	62.919	-12.583	225.4	±65.310	334.94
12	55.965	-11.19	70.178	-14.035	256.7	±74.40	382.84
13	61.320	-12.26	74.283	-14.856	276.7	±80.193	403.283
14	64.890	-12.98	76.160	-15,232	280.6	±56.12	421.65
15	64.995	-12.99	76.866	-15.373	280.6	±56.12	422.356

16	64.890	-12.98	77.101	-15.420	280.6	±56.12	422.696
17	64.995	-12.99	77.218	-14.443	280.6	±56.12	422.818
18	65.100	-13.02	77.220	-15.444	280.6	±56.12	422.92
19	64.050	-12.81	77.220	-15.444	280.6	±56.12	421.87
20	62.370	-12.47	77.220	-15.444	280.6	±56.12	420.19
21	62.160	-12.43	77.220	-15.444	280.6	±56.12	419.98
22	61.950	-12.39	77.220	-15.444	280.6	±56.12	419.72
23	60.900	-12.18	77.220	-15.444	280.6	±56.12	418.7
24	60.375	-12.075	77.220	-15.444	280.6	±56.12	418.18
25	59.850	-11.97	77.220	-15.444	280.6	±56.12	417.65

Table 5: Bus Result for Canal Zone 34 –Bus System at rated wind speed

Bus No	Bus Code	Bus Name	Voltage Mag.	Voltage Degree	Load		Generators MVA	
					MW	Mvar	MW	Mvar
1	Slack	Ayoun Mousa	1.025	0.0	245	105	0.0	0.0
2	PQ	Suez 500	0.996	3.125	0.0	0.0	0.0	0.0
3	PV	Ataka P.S.	0.995	4.231	0.0	0.0	780	425
4	PQ	Suez 2	1.013	-2.125	155	65	0.0	0.0
5	PV	Suez thermal	1.023	4.542	90	40	80	0.0
6	PQ	Arouk Elsoulb	0.995	-5.234	100	40	0.0	0.0
7	PQ	Suez-Cement	0.992	6.536	110	40	0.0	0.0
8	PQ	Al-Sokhna	0.994	-4.872	140	50	0.0	0.0
9	PV	Zafrana	0.995	5.997	0.0	28.5	425	50
10	PQ	Al-Ektsadia	1.012	-3.875	120	50	0.0	0.0
11	PV	Gulf Power Station	1.025	5.987	0.0	0.0	680	315
12	PQ	El_Ezz	1.005	3.125	280	105	0.0	0.0
13	PQ	Arabia Cement	0.991	4.231	30	30	0.0	0.0
14	PQ	Masria Cement	1.010	-2.125	120	60	0.0	0.0
15	PV	Abo Sultan PS	0.997	4.542	0.0	0.0	550	240
16	PQ	New El_Asher	0-.997	-5.234	205	110	0.0	0.0
17	PQ	El_Asher 220	0.996	6.536	140	105	0.0	0.0
18	PQ	El_Mnaief	1.011	-4.872	210	115	0.0	0.0
19	PQ	Zagazig	0.955	3.997	0.0	0.0	0.0	0.0
20	PQ	New Sharkia	1.012	-3.875	260	135	0.0	0.0
21	PQ	Raswa	0.993	6.125	170	105	0.0	0.0
22	PV	Port Said Boot	1.015	4.231	0.0	0.0	600	335
23	PQ	Peer El_Abd	1.011	-2.125	200	90	0.0	0.0
24	PV	Arish PS	0.995	4.542	60	40	0.0	0.0
25	PQ	East Kantara	0.904	-5.234	210	110	0.0	0.0
26	PQ	Taba 500	1.011	6.536	300	120	0.0	0.0
27	PQ	Nuwebaa	0.995	-4.872	120	50	0.0	0.0
28	PV	Sharm PS	1.015	2.997	280	110	125	0.0
29	PQ	Trust	0.994	-3.875	100	40	0.0	0.0
30	PQ	Hurgada	1.023	5.987	200	95	0.0	0.0
31	PQ	Safaga	1.032	3.125	0.0	0.0	0.0	0.0
32	PQ	Suez 500	0.954	4.231	0.0	0.0	0.0	0.0
33	PV	Ayoun Mousa	1.011	-2.125	30	10	0.0	0.0
34	PQ	Taba 500	0.995	5.345	0.0	0.0	0.0	0.0

Table 6: Line Result for Canal Zone 34 –Bus System

From	To	Line Flow (MVA)	Capacity MVA	No. of Circuits.
1	2	900	1040	2
1	26	550	1040	1
1	33	410	500	-----
2	32	380	500	-----
3	32	210	2*305	2
3	6	180	2*229	2
3	14	310	2*286	2
3	4	328	2*229	2
3	7	280	2*229	2
4	5	310	2*229	2
4	32	220	2*305	
7	8	240	2*229	2
8	10	380	2*246	2
8	9	310	2*305	2
10	11	328	2*305	2
11	12	280	2*305	2
12	13	260	2*286	2
13	14	220	2*305	2
15	16	210	2*286	2
15	18	180	2*248	2
15	32	310	2*248	2
16	17	328	2*248	2
16	20	280	2*248	2
18	19	260	2*248	2
18	20	220	2*305	2
18	21	210	2*248	2
20	22	180	2*305	2
21	22	310	2*305	2
22	23	328	2*305	2
21	29	280	2*305	2
23	24	220	2*286	2
23	25	220	2*305	2
25	33	180	2*305	2
27	28	180	2*305	2
27	34	300	2*305	2
30	31	350	2*286	2

5. Impact of Zafarana Wind Farm on Voltage Stability of the Canal Zone

An area of 8 buses of the Canal Zone is taken for studying briefly the load flow surround Zafarana wind farm and the impact of the farm on the specified area as shown in Fig. 10 at base case.

5.1. Sensitivity Analysis for Canal Zone

At each load bus of the studied system, the reactive power is increased till reaching the collapse point of the system. The reactive power difference between collapse point and first loading point is defined as stability margin which is taken as an index of voltage stability. Table 7 shows the result of the voltage stability sensitivity analysis for Canal Zone where Zafarana wind farm operated at rated power (rated wind speed). As shown from the table, the most sensitive bus in the system is bus 13. Increasing the load at that bus leads the system to collapse faster than any other bus.

5.2. Voltage Stability Analysis

In this section probabilistic voltage stability study of WTGUs interconnected with the Egyptian utility grid is developed via power flow analysis. The WTGUs are modeled as P-Q bus (es) in case of fixed speed and P-V bus (es) in case of variable speed unit by detecting the collapse point on the Q-V curves. The probabilistic nature of wind is considered by introducing the expected voltage stability margin as an index that combines both of the voltage stability and the wind distribution in one index.

As explained before (section 5.1), the difference of the reactive power between collapse point and first loading point is defined as stability margin. This margin is taken as an index of voltage stability to evaluate the influence of wind farm on the system voltage stability analysis. The following equations are used to determine the voltage stability margin considering the probabilistic nature of the wind [19]:

$$\mathrm{EVSM}_v = p_\upsilon * \mathrm{VSM}_v \tag{19}$$

$$\mathrm{VSM} = \sum_{all\ speed} \mathrm{EVSM}_\upsilon \tag{20}$$

Where

p_υ : probability of speed υ
VSM_υ: voltage stability margin at speed υ
VSM : system voltage stability margin
EVSM: expected voltage stability margin at speed υ

5.3. Impact of WTGUs on Voltage Stability of the Canal Zone

For most sensitive bus in the system (bus 13), the voltage stability margin at each individual wind speed is calculated by detecting the collapse point. Then the expected voltage stability margin of the system is calculated as a function of wind speed and the expected voltage stability margin of the system is then calculated using equations 19 and 20.

Voltage stability assessment for Canal Zone after wind farm interconnection is explained by Table 8. The final value of the expected voltage stability margin (EVSM) for the Canal Zone including Zafarana wind farm applied to the most sensitive bus is illustrated in the table as relevant value to the wind farm with total capacity.

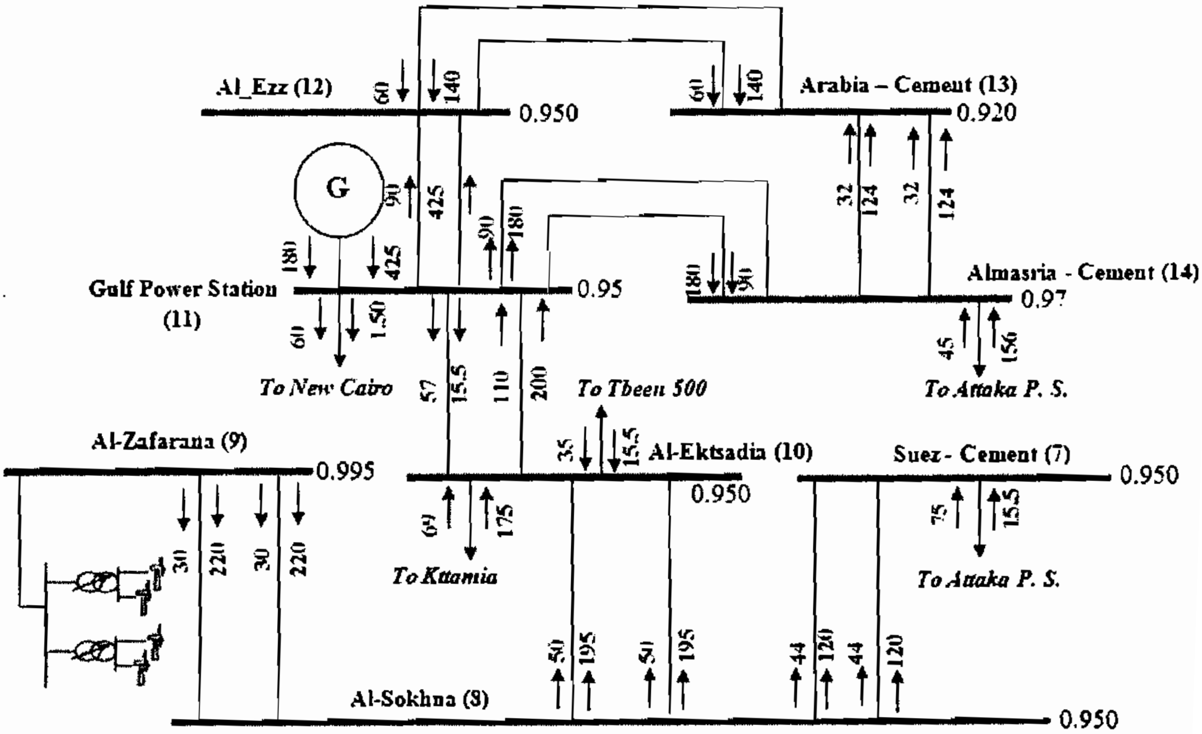

Fig. 10: Base case for Canal Zone (The part nearby Zafarana wind farm)

Table 7: Sensitivity Analysis of Canal Zone

Load Bus No	**Load MVar**	**Collapse points**		**Stability Margin (MVar)**
		Voltage Magnitude (pu)	**Reactive Power (MVar)**	
2	175	0.469	877	319
4	185	0.526	735	735
6	0	0.589	975	2975
8	150	0.453	555	225
10	120	0.498	528	432
12	170	0.543	645	615
13	30	0.596	207	197
14	70	0.526	465	395
16	110	0.497	415	305
17	200	0.608	718	518
18	134	0.428	439	305
19	200	0.546	710	510
20	115	0.561	430	315
21	110	0.587	440	330
23	100	0.489	386	286
23	60	0.526	280	220
25	54	0.617	340	286
26	26	0.509	296	270
27	50	0.526	465	415
29	100	0.543	510	410
30	150	0.547	620	470
31	45	0.489	286	241

Table 8: Voltage Stability Assessment for Canal Zone after Wind Farm Interconnection

Wind Speed (m/s)	Probability P_υ	Collapse Point		Voltage Stability Margin (VSM_υ)	$EVSM_\upsilon$
		Voltage	MVAr		
4	0.009	0.411	55	25	0.0
5	0.0156	0.439	62	31	0.484
6	0.13447	0.457	70	43	5.782
7	0.02217	0.471	79	61	19.94
8	0.1542	0.497	88	71	10.94
9	0.17374	0.510	99	61	10.37
10	0.11986	0.515	107	77	8.47
11	0.10011	0.528	125	95	9.500
12	0.08972	0.536	140	110	9.440
13	0.15868	0.570	169	139	8.579
14	0.05628	0.573	188	158	6.714
15	0.04852	0.574	193	163	5.542
16	0.02454	0.574	197	167	2.865
17	0.01073	0.573	200	170	1.8691
18	0.00776	0.574	201	171	0.6596
19	0.00308	0.577	205	175	0.2679
20	0.00103	0.575	207	177	0.09
21	0.00023	0.573	207	177	0.011
22	0.00011	0.576	207	177	0.01
24	0.00011	0.577	207	177	0.01
25	0	----	0	0	0
Total	1				##

As seen in Table 8, the voltage stability assessment applied on Bus 13 as illustrated in Table 7 at which its collapse point is 207 MVar in case of full wind farm capacity (425 MW). The table shows that: at high wind speed the results are acceptable while at low wind speed it should be considered.

6. Conclusion

Modeling algorithms for fixed speed wind turbines with SCIG and Variable speed wind turbines with DFIG were developed and applied to Zafarana wind farm to study the impact of the WTGU on the Egyptian utility grid. The total active and reactive power delivered from Zafarana wind farm according to its different control strategies which either fixed speed with its two types (stall regulated or pitch regulated) or variable speed at all wind speed range from cut-in speed to cut-out speed are developed. The derived models are verified using the actual data measured from the site as a very good approximation. So, the models are used for further analysis to measure the effect of Zafarana wind farm on the Egyptian grid.

The proposed models are simulated through power flow program to study the impact of Zafarana wind farm on the Canal Zone (one of the five Egyptian utility grid zones). Also, there is a new approach to calculate the system voltage stability margin that incorporate the voltage stability margin at each wind speed and the probability of the occurrence of this speed by accumulating for all expected wind speeds.

The method used in modeling and simulating Zafarana wind farm is general and can be applied to other wind farms. The proposed method is suitable and convenient to be implemented on wind farms as well as any other renewable or intermittent supply as it uses a general and comprehensive approach.

7. References

1. G. Slooteg, S. Haan, H. Polinder and W. Kling, "*Modeling Wind Turbines in Power System Dynamic Simulations*", IEEE Trans. Power Systems. Vol. 7, pp. 22-26, 2001.
2. T. Petru, "*Modeling of Wind Turbine for Power System Studies*" Ph. D. Thesis, Department of Electrical Power Engineering, Chalmers University of Technology, Sweden 2003.
3. F. Iov, A. Hansen, P. Sorensen and C. Petru, "*Advanced Tools for Modeling, Design and Optimization of Wind Turbine System*" Nordic Wind Power Conference, Chalmers University of Technology, March ,2004.
4. P. Sorensen, A. Hancen, L. Janosi and B. Bak-Jensen, "*Simulation of Interaction between Wind Farm and Power System*" Riso-R-1281(EN), Riso National Laboratory, Roskilde, December 2003.
5. M. Fernandez, J. Saenz and F. Jurado "*Dynamic Models of Wind Farms With Fixed Speed Wind Turbines*" Renewable Energy, Vol. 31, 2006, pp. 1203- 1230.
6. J. G. Slooteg, H. Polinder and W.L. Kling, "*General Model for Presenting Variable Wind Speed Turbines in Power System Dynamic Simulations*", IEEE Trans. Power Systems, Vol. 18, No1, February 2003.
7. J. Pierik, J. Morren and S. Haan "*Dynamic Models of Wind Farms for Grid Integration Studies*" Nordic Wind Power Conference, Chalmers University of Technology, March 2004.
8. K.C. Divya and P.S. Nagevdra Rao "*Models for Wind Turbine Generating Systems and their Application in Load Flow Analysis*", ELSEVIER, Electric

Power Systems Research, Vol. 18, No. 3, pp. 249-262, October 2005.

9. A. Hansen, P. Sorensen and J. Blaabjerg *"Dynamic Modeling of Wind Farm Grid Interaction"* Wind Engineering, Volume 26, No.4, pp191-208, 2002.

10. H. Holttinen, P. Meibom and C. Ensslin "Design *and Operation of Power Systems with Large Amount of Wind Power*", Nordic Wind Power Conference, Espoo, Finland, May 2006

11. T. Ackermann "*Wind Power in Power Systems*", book, John Wiley & Sons Ltd, Royal Institute of Technology, Stockholm, Sweden, 2005.

12. A. Feijo and J. Cidras *"Modeling of Wind Farms in Load Flow Analysis"* IEEE Transactions on Power Systems, Vol. 15, No. 1, February, 2000.

13. G. Slootweg, H. Polinder and W. Kling "*Dynamic Modeling of a Wind Turbine with Doubly Fed Induction Generator*", IEEE Transactions on Power Systems, Vol. 11 No. 2, March 2001.

14. A. Pettersson *"Analysis, Modeling and Control of Doubly Fed Induction Generators for Wind Turbines"*, Ph. D. Thesis, Department of Electrical Power Engineering, Chalmers University of Technology, Sweden 2005.

15. M. Z. El-Sadek, "*Power Systems Voltage Stability and Power Quality*", book, Mukhtar Press, 2003.

16. Egyptian New and Renewable Energy Association, NREA Annual Report, 2009, *http://www.nrea.gov.eg/annual-english-2008-2009.pdf*

17. General Specifications-Gamesa Wind Systems,G850/52-850KW, *www.Gamesa.com*

18. Egyptian Electricity Holding Company Annual Report 2008/2009 *http://www.moee.gov.eg/English/Electric eng 2010.pdf*

19. C. A. Canizares, Editor, *"Voltage Stability Assessment, Procedures and Guides"*, IEEE/PES Power Systems Stability Subcommittee, Jan. 1999.

Appendix

Canal Zone bus and line Data

Table A1 Bus Data of Canal Zone 34-Bus System [18]

Bus No	Bus Code	Bus Name	Voltage (pu)	Angle (degree)	Load		Generator				Generators MVA	Transformers MVA
					MW	Mvar	MW	Mvar	Qmin	Qmax		
1	Slack	Ayoun Mousa	1.025	0.0	245	105	0.0	0.0	0.0	0.0	2*395	1*500
2	PQ	Suez 500	1.0	0.0	0.0	0.0	0.0	0.0	0.0	0.0	—	1*500
3	PV	Ataka P.S.	0.995	0.0	0.0	0.0	900	0.0	50	650	2*410+2*185	—
4	PQ	Suez 2	1.0	0.0	155	65	0.0	0.0	0.0	0.0	—	3*125
5	PV	Suez Thermal	1.0	0.0	90	40	97	0.0	0.0	55	1*114	2*60
6	PQ	Arouk Elsoulb	1.0	0.0	100	40	0.0	0.0	0.0	0.0	—	1*105+1*15
[illegible]	[illegible]	[illegible]	[illegible]	[illegible]	[illegible]	[illegible]	[illegible]	[illegible]	[illegible]	0.0	—	2*75
[illegible]	[illegible]	[illegible]	[illegible]	[illegible]	[illegible]	[illegible]	[illegible]	[illegible]	[illegible]	0.0	—	3*60
[illegible]	[illegible]	[illegible]	[illegible]	[illegible]	[illegible]	[illegible]	[illegible]	[illegible]	[illegible]	[illegible]	[illegible]	—
[illegible]	[illegible]	[illegible]	[illegible]	[illegible]	[illegible]	[illegible]	[illegible]	[illegible]	[illegible]	0.0	—	2*75
[illegible]	[illegible]	[illegible]	[illegible]	[illegible]	[illegible]	[illegible]	[illegible]	[illegible]	[illegible]	[illegible]	[illegible]	—
[illegible]	[illegible]	[illegible]	[illegible]	[illegible]	[illegible]	[illegible]	[illegible]	[illegible]	[illegible]	0.0	—	2*200
[illegible]	[illegible]	[illegible]	[illegible]	[illegible]	[illegible]	[illegible]	[illegible]	[illegible]	[illegible]	[illegible]	—	3*35
[illegible]	[illegible]	[illegible]	[illegible]	[illegible]	[illegible]	[illegible]	[illegible]	[illegible]	[illegible]	0.0	—	3*90
[illegible]	[illegible]	[illegible]	[illegible]	[illegible]	[illegible]	[illegible]	[illegible]	[illegible]	[illegible]	200	[illegible]	—
16	PQ	New El Asher	1.0	0.0	205	110	0.0	0.0	0.0	0.0	—	2*125
17	PQ	El Asher 220	1.0	0.0	140	105	0.0	0.0	0.0	0.0	—	4*125

18	PQ	El_Mnaief	1.0	0.0	210	115	0.0	0.0	0.0	0.0	——	2*125
19	PQ	Zagazig	1.0	0.0	0.0	0.0	0.0	0.0	0.0	0.0	——	4*125
20	PQ	New Sharkia	1.0	0.0	260	135	0.0	0.0	0.0	0.0	——	2*125
21	PQ	Port Said Raswa	1.0	0.0	170	105	0.0	0.0	0.0	0.0	——	2*125
22	PV	Port Said Boot	1.015	0.0	0.0	0.0	640	0.0	40	400	2*420	——
23	PQ	Peer El_Abd	1.0	0.0	200	90	0.0	0.0	0.0	0.0	——	2*125+2*40
24	PV	Arish PS	0.995	0.0	60	40	0.0	0.0	0.0	0.0	2*45	2*40
25	PQ	East Kantara	1.0	0.0	210	110	0.0	0.0	0.0	0.0	——	2*125
26	PQ	Taba 500	1.0	0.0	300	120	0.0	0.0	0.0	0.0	——	1*500+1*750
27	PQ	Nuwebaa	1.0	0.0	120	50	0.0	0.0	0.0	0.0	——	2*75
28	PV	Sharm PS	1.015	0.0	280	110	146	0.0	20	80	3*20+2*25	3*125
29	PQ	Trust	1.0	0.0	100	40	0.0	0.0	0.0	0.0	——	2*125
30	PQ	Hurgada	1.0	0.0	200	95	0.0	0.0	0.0	0.0	——	3*125
31	PQ	Safaga	1.0	0.0	0.0	0.0	0.0	0.0	0.0	0.0	——	1*125
32	PQ	Suez 500	1.0	0.0	0.0	0.0	0.0	0.0	0.0	0.0	——	——
33	PV	Ayoun Mousa	1.0	0.0	30	10	0.0	0.0	0.0	0.0	——	1*40
34	PQ	Taba 500	1.0	0.0	0	0	0.0	0.0	0.0	0.0	——	——

Table A2 Line Data of Canal Zone 34 Bus System [18]

From	To	R	X	B	Line Code	Length (km)	Capacity MVA	No of Circuits
1	2	0.0011	0.0154	0.0474	1	23.3	1040	2
1	26	0.0049	0.0269	0.241	1	244	1040	1
1	33	0.0	0.0043	0.0	2.27	——	500	——
2	32	0.0	0.542	0.0	2.27	——	500	——
3	32	0.0011	0.0144	0.0462	1	14	2*305	2
3	6	0.0035	0.0367	0.0160	1	3	2*229	2
3	14	0.0035	0.0523	0.0162	1	60	2*286	2
3	4	0.0035	0.0967	0.0161	1	10	2*229	2
3	7	0.0035	0.0267	0.0262	1	54	2*229	2
4	5	0.001	0.0051	0.0079	1	6	2*229	2
4	32	0.0035	0.0467	0.0160	1	5	2*305	
7	8	0.0024	0.0461	0.0160	1	27	2*229	2
8	10	0.0015	0.0962	0.0262	1	2	2*246	2
8	9	0.0035	0.0967	0.0160	1	56	2*305	2
10	11	0.0005	0.0464	0.0326	1	4.7	2*305	2
11	12	0.0035	0.0968	0.0162	1	15	2*305	2
12	13	0.0011	0.0661	0.0132	1	25	2*286	2
13	14	0.0035	0.0867	0.0162	1	7	2*305	2
15	16	0.0035	0.0967	0.0162	1	57.5	2*286	2
15	18	0.0035	0.0153	0.0562	1	40	2*248	2
15	32	0.0017	0.0967	0.0261	1	74.5	2*248	2
16	17	0.0035	0.0961	0.0162	1	22.5	2*248	2
16	20	0.0025	0.0867	0.0164	1	55.5	2*248	2
18	19	0.0035	0.0964	0.0162	1	59	2*248	2
18	20	0.0017	0.0563	0.0132	1	46	2*305	2
18	21	0.0019	0.0967	0.0172	1	63	2*248	2
20	22	0.0025	0.0964	0.0465	1	100	2*305	2
21	22	0.0035	0.0962	0.0268	1	64	2*305	2
22	23	0.0035	0.0567	0.0162	1	61.8	2*305	2
21	29	0.0035	0.0967	0.0162	1	3.5	2*305	2
23	24	0.0033	0.0461	0.0261	1	65	2*286	2
23	25	0.0035	0.0467	0.0162	1	68	2*305	2
25	33	0.0025	0.0763	0.0162	1	120	2*305	2
27	28	0.0035	0.0969	0.0324	1	152	2*305	2
27	34	0.0005	0.0964	0.0360	1	105	2*305	2
30	31	0.0015	0.0967	0.0162	1	43	2*286	2